

Mapping enzymatic functionalities of mannuronan C-5 epimerases and their modular units by dynamic force spectroscopy

Marit Sletmoen,^a Gudmund Skjåk-Bræk^b and Bjørn T. Stokke^{a,*}

^a*Biophysics and Medical Technology, Department of Physics, The Norwegian University of Science and Technology, NTNU, NO-7491 Trondheim, Norway*

^b*Norwegian Biopolymer Laboratory (NOBIOL), Department of Biotechnology, The Norwegian University of Science and Technology, NTNU, NO-7491 Trondheim, Norway*

Received 3 April 2005; received in revised form 26 September 2005; accepted 28 September 2005

Available online 24 October 2005

Abstract—Alginates are (1→4)-linked structural copolyuronans consisting of β-D-mannuronic acid (M) and its C-5 epimer α-L-guluronic acid (G). The residue sequence variation is introduced in a unique postpolymerisation step catalysed by a family of C-5 epimerases named AlgE enzymes. The seven known AlgE's are composed of two modules, designated A and R, present in different number. The molecular details of the structure–function relationship of these seven epimerases, introducing specific residue sequences, are not understood. In this study, single-molecular pair interactions between alginate and AlgE enzymes were investigated using dynamic force spectroscopy. The AlgE enzymes AlgE4 and AlgE6, the recombinant construct PKA1 composed of A- and R-modules from various AlgE's, as well as separate R- and A-modules were studied. The strength of the protein–mannuronan interaction, when applying a loading rate of 0.6 nN/s, varied from 73 pN (AlgE4) to 144 pN (A-module). The determined potential width, that is, the distance from the activation barrier to the bound substrate molecule, was 0.23 nm for AlgE4, 0.19 nm for AlgE6 and 0.1 nm for the A-module. No attraction was observed between the R-module and the substrate. The observations indicate that the A-module contains the substrate binding site and that the R-module modulates the enzyme–substrate binding strength. The observed AlgE4-polymer residence times, two orders of magnitude longer than expected from k_{cat} reported for AlgE4, not observed for PKA1, led us to propose a processive mode of action of AlgE4.

© 2005 Elsevier Ltd. All rights reserved.

Keywords: Alginate; Epimerase; AFM; Single-molecule; Force spectroscopy; Mode of action

1. Introduction

Molecular monolayers, including layers of functional biological macromolecules, which retain their function in the immobilised state on solid surfaces, are important in material science, analytical detection and other technology approaching the nanoscale. Studies of such layers have offered new insight into the functional properties and single-molecular features. Results obtained so far using AFM include high-resolution images of DNA,¹ proteins,² or living cells adsorbed on biomaterials.³ In addition to the powerful imaging capabilities of

the AFM, it also provides a tool for measuring and mapping forces with high spatial resolution. This methodology has allowed studies of surface properties as, for example, hardness, friction or elasticity⁴ or localisation of specific receptors on that is the cell surface.⁵ Recently, the focus of many AFM based experiments has shifted to direct measurement of the force required to separate molecules making up molecular complexes. To measure intermolecular forces with AFM, the AFM tip is functionalised in order to exhibit the desired material and chemical properties at its surface. The molecules exposed on the surface of the tip are then allowed to interact with other molecules, which are often immobilised by selective binding to a surface. Pulling experiments in which the tip–surface separation speed is changed in such a way that the force per unit time acting on the

* Corresponding author. Tel.: +47 73 59 34 34; fax: +47 73 59 77 10; e-mail: bjorn.stokke@phys.ntnu.no


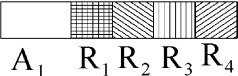


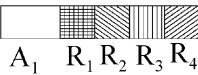


molecular bond under study is changed over many orders of magnitude, are referred to as dynamic force spectroscopy.^{6,7} This experimental set-up opens for studies of the mechanics of biological interactions that is the influence of force on structural stability, conformational transitions, intermolecular interactions and single-molecule *function*, and therefore represents the ultimate limit for biochip analysis. Examples of studies performed using this technique include the study of complexes formed between complementary strands of DNA,⁸ biotin and avidin,⁹ antigens and antibodies,¹⁰ carbohydrates and lectins,^{5,11} glycan polysaccharides,¹² as well as numerous studies of mechanical induced conformational changes¹³ or unfolding mechanics of proteins.¹⁴

The present study describes single-molecule dynamic force spectroscopy applied to determine the strength and the energy landscape of the interaction between alginate polysaccharides and the structurally similar, but functionally different AlgE4 and AlgE6 epimerases (Table 1). Alginates are structural copolyuronans consisting of (1→4)-linked residues of β-D-mannuronic acid (M) and α-L-guluronic acid (G) (Fig. 1). They are ubiquitous in the extracellular part of brown algae and are secreted by bacteria of the *Azotobacter* and *Pseudomonas* genera.¹⁵ The composition of the polymers vary from 100% M (polyM, also referred to as mannuronan) to more than 70% G. Naturally occurring alginates are composed of regions of M and G, termed M- and G-

blocks, of varying length, interspersed with regions of alternating structure (MG-blocks). This sequence, which is non-random and which cannot be described by Bernoullian statistics, is introduced in a postpolymerisation epimerisation of a fraction of the M units. This epimerisation is catalysed by a family of mannuronan C-5 epimerases, the AlgE's.

The *Azotobacter vinelandii* genome encodes seven evolutionary related and Ca²⁺-dependent C-5 epimerases (AlgE1-7). All seven enzymes have been sequenced, cloned and expressed at high levels and in active forms in *Escherichia coli*.¹⁶ The reaction products obtained after exposing polyM alginate to these enzymes are highly dependent on the enzyme (Table 1). AlgE4 and AlgE6 may be seen as the extreme examples, as observed by NMR spectroscopy. AlgE4 generates predominantly an alternating residue sequence, a pattern, which does not allow gel-formation in aqueous Ca²⁺-containing solutions. AlgE6 introduces long stretches of G (G-blocks) and the content of G in the product can reach 78%.¹⁶ Such polymer-products support gel formation by complexation with Ca²⁺. AlgE2 and AlgE5 generate shorter G-blocks than AlgE6, while AlgE1 and AlgE3 both display two distinct catalytic activities, one generating G-blocks and the other alternating sequences.¹⁶ AlgE7 is clearly different from all the others, in that it displays both epimerase and lyase activity.¹⁷ By modulating the expression levels of the different AlgE

Table 1. The modular structure and epimerisation patterns of AlgE epimerases

Epimerase	Modular structure	Epimerisation pattern				
		F_G	F_{GG}	$F_{MG,GM}$	$N_{(G>1)}^a$	F_G/F_M
AlgE1	 A ₁ R ₁ R ₂ R ₃ A ₂ R ₄	0.47	0.23	0.25	8.5	1.9
AlgE2	 A ₁ R ₁ R ₂ R ₃ R ₄	0.63	0.45	0.18	7.4	3.5
AlgE3	 A ₁ R ₁ R ₂ R ₃ A ₂ R ₄ R ₅ R ₆ R ₇	0.65	0.46	0.19	9.0	3.4
AlgE4	 A ₁ R ₁	0.36	0.04	0.33		1.1
AlgE5	 A ₁ R ₁ R ₂ R ₃ R ₄	0.43	0.28	0.15	5.8	2.9
AlgE6	 A ₁ R ₁ R ₂ R ₃	0.78	0.57	0.21	15	3.7
AlgE7	 A ₁ R ₁ R ₂ R ₃	0.34	0.09	0.25		1.4

The A- and R-modules are grouped based on sequence alignments,^{16,17} as indicated by the different patterns.

^a Mean G block length: $N_{(G>1)} = (F_G - F_{MG,GM})/F_{GG}$, if F_{GG} is below 0.1, this parameter cannot be accurately calculated.

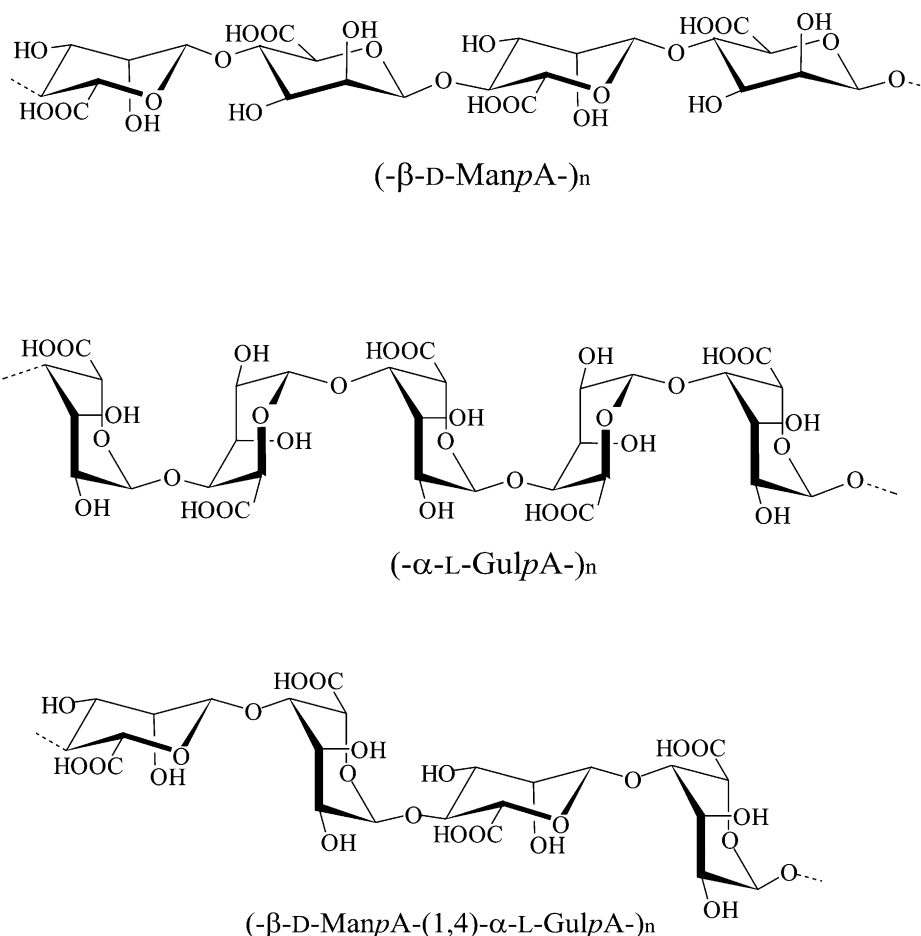


Figure 1. Block structures of polyuronic acids: (1→4) linked residues of β-D-mannuronic acid (polyM), (1→4)-linked residues of α-L-guluronic acid (polyG) and (1→4)-linked alternating sequence of β-D-mannuronic acid and α-L-guluronic acid (polyMG).

enzymes, *A. vinelandii* cells control the viscoelastic properties of their polysaccharide secretions. In the same way, recombinantly produced AlgE enzymes can be used as tools for controlled modification of alginates.¹⁸

The AlgE enzymes are all composed of two structurally distinct protein modules, designated A and R. The A-modules are present in one or two copies in each enzyme (Table 1). This module contains the alginate binding site¹⁹ and is sufficient for epimerisation, although the observed reaction rates for A-modules alone are low compared to what is observed for the intact AlgE's containing R-module.¹⁹ The R-module is present in one to seven copies. It contains a residue motif, which resembles Ca²⁺-binding motifs found in other proteins,¹⁶ and both A- and R-modules bind this ion in vitro. Such modular structure is unusual for bacterial proteins, and the nature of the structure/function relationships is not understood at a molecular level. The differences in the pattern of G-units introduced in the mannuronan substrate by the enzymes are to some extent reflected at the amino-acid sequence level of their A-modules. On this basis, the A-modules have been classified into three groups.^{17,20} The ones known to generate alternating

sequence structures in their substrates belong to one group. Interestingly, this group also includes the A-module present in AlgE6, an enzyme capable of generating very long G-blocks. The classification based on sequence alignments, therefore, does not conclusively reflect the biochemical properties of the enzymes.

Any enzyme that has more than one substrate-binding subsite, and performs multiple modifications on the substrate, may display processivity. Enzyme processivity is a measure of the average number of times a reaction is repeated between association and dissociation of an enzyme–substrate complex. The polymer modifying enzymes involved in the biosynthesis of the glycosaminoglycans heparin and heparan sulfate are supposed to act in a processive fashion.²¹ For the alginate case, the formation of long blocks (MG or GG) can be explained by either a high degree of processivity, or by a preferred attack mechanism. The alternating MG sequence observed in polyM converted by AlgE4 has been taken to indicate a non-random, possibly a processive mode of action for this enzyme.²² In a recent study, involving specific degrading enzymes, NMR, electrospray ionisation mass spectrometry (ESI-MS) and capillary

electrophoresis, it was shown that on average 10 residues are epimerised for each AlgE4 substrate encounter.²³ This methodology, combined with the use of ¹³C-labelled mannuronan oligomers as substrate for the epimerase, allowed identification of a hexameric oligomer as the minimum substrate chain length needed to accommodate activity.

Here, dynamic force spectroscopy is applied to determine the interaction between selected AlgE epimerases and their substrate, as well as to address questions concerning the structure to function relationship and the mode of action of these enzymes. The method employed for covalent binding of polysaccharides and enzymes to functionalised mica substrates or atomic force microscope (AFM) tips was characterised and optimised.

2. Experimental procedures

2.1. Materials

2.1.1. Polysaccharides. High molecular weight polyM alginate was produced by growing an epimerase negative (AlgG[−]) mutant of *Pseudomonas fluorescens*, and was provided by SINTEF, Applied Chemistry (Trondheim, Norway). The weight average molecular weight of the polyM sample, determined by SEC-MALLS,^{24,25} was $M_w = 645$ kDa. The sample depicted PolyMG alginate was prepared from polyM by epimerisation with AlgE4, giving a product with a fraction of G, F_G of 0.46. The commercial alginate used had been extracted from the leaf of *Laminaria hyperborea*. The composition and sequence parameters of this alginate has earlier been determined to $F_G = 0.55$, fraction of M to be $F_M = 0.45$ and the three fractions of diad combinations $F_{GG} = 0.38$, $F_{MM} = 0.28$ and $F_{GM, MG} = 0.17$.¹⁵ The sample used had a M_w equal to 455 kDa. The extracellular polysaccharide xanthan was produced by fermentation of *Xanthomonas campestris*. The polysaccharide fraction of the fermentation broth (Statoil, Bioferm) had been cleaned and isolated by centrifugation, precipitation and filtration and was dissolved in 0.1 M NaCl.

2.1.2. Proteins. The C-5 epimerase AlgE4, $M = 57.7$ kDa, was produced by fermentation of recombinant strains of *E. coli*, JM 105²⁰ and partly or highly purified by ion exchange chromatography on Q-Sepharose FF followed by hydrophobic interaction chromatography on Phenyl Sepharose FF (Pharmacia, Uppsala, Sweden).²² The AlgE4-A-module was produced from a truncated derivative of AlgE4 in which the R-module had been removed at the DNA level. To express and purify this A-module, the IMPACT-CN system from New England Biolabs was used. The R-module was produced by transferring genes coding for the R-module to *E. coli* cells. A fusion protein, verified to be the R-mod-

ule, was expressed by the genetic modified *E. coli* cells.²⁶ The hybrid epimerase PKA1 was produced similarly.²⁷ AlgE6 was produced using *E. coli* strain SURE carrying the plasmid pBG27 as previously described.¹⁷ BSA was obtained from Sigma.

2.1.3. Chemicals. Glutaraldehyde was obtained from Sigma–Aldrich. The other reagents used were supplied by Acros organics. The MQ-water used had a resistivity equal to 10.3 MΩ cm.

2.2. Methods

2.2.1. Surface immobilisation of enzymes. Recombinantly produced AlgE4, AlgE6 as well as the A- and R-modules of these enzymes were immobilised on separate mica surfaces. The immobilisation procedure used included silanisation, attachment of coupling agent (glutaraldehyde) and protein conjugation to unreacted aldehyde groups of glutaraldehyde (Fig. 2) as described.²⁸ Mica surfaces covered with BSA, used to test the specificity of the measured interaction were prepared using the same immobilisation strategy. Additionally, the AlgE4 preparation was in some of the experiments blended with a 1 mg/mL stock solution of BSA prior to the enzyme conjugation step in order to reduce the surface density of epimerases. The mass ratio of the two proteins, that is, $m_{\text{AlgE4}}/m_{\text{BSA}}$, where m_{AlgE4} is the mass of AlgE4 and m_{BSA} the mass of BSA added to the solution, was 0.1. The total mass of protein added was the same as in the procedure involving only AlgE enzymes.

2.2.2. Dynamic contact angle measurements. The contact angle, θ , between water and mica was determined in order to characterise the surface properties at the various stages of the immobilisation procedure of mica (1 cm × 1 cm) using a Sigma 70 tensiometer. The surface reaction had proceeded on both sides of the mica slide. The surface tension of the liquid used (MOPS (3-[N-morpholino]propanesulfonic acid) pH 6.8) was measured using a Du Nouy ring, which was moved up and down by a speed equal to 10.0 mm/min. The immersion depth was 5 mm and data were collected starting from 2.5 mm below the surface. The mica slides were placed on the balance and tarred. The force acting on the balance was recorded as the slides were immersed into the liquid. The wetting force is a product of the liquid

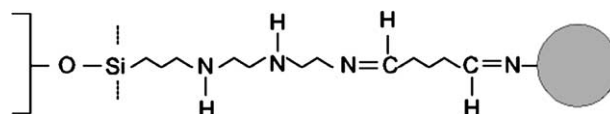


Figure 2. Schematic illustration of functionalised mica slides. Freshly cleaved mica was cleaned, silanised and functionalised as described in the text to give surfaces covered with covalently bound active proteins (depicted as grey sphere).

surface tension, a perimeter of the probe and the contact angle. In order to obtain this force from the total force acting on the balance, the weight of the probe was subtracted and the effects of the buoyancy force removed by extrapolating the graph back to zero depth of immersion.

2.2.3. Tip-functionalisation. The carboxylate group of the polysaccharides employed was utilised for covalent attachment to the AFM tips. The SiO_x layer of the standard commercially available Si_3N_4 cantilever (Veeco Instruments) was silanised using the same silanisation reagent as for the mica surface.^{29,30} Subsequently, the amine group of the silanisation reagent was coupled to the carboxyl group of the polysaccharide using the water soluble coupling agent *N*-ethyl-*N'*-(3-dimethylamino-propyl) carbodiimide hydrochloride (EDAC).³¹ EDAC was added to a solution of alginate (20 $\mu\text{g}/\text{mL}$) dissolved in 50 mM boric acid pH 5.8, to give a final concentration of EDAC of 0.5–1.0 mg/mL. The tip was left in contact with this solution at room temperature for

1–14 h, transferred to MQ-water and stored until used. Xanthan-functionalised tips used to test the specificity of the measured interaction were prepared using the same reaction (20 μg xanthan/mL 50 mM boric acid). Contact mode AFM tips with nominal force constant $k = 0.06 \text{ nN}/\text{nm}$ functionalised with polysaccharide chains were calibrated using the equipartition method.³²

2.2.4. Atomic force microscopy. AFM topographs of the mica surfaces at different steps in the immobilisation process were obtained using a Digital Instrument Multi-mode IIIa atomic force microscope equipped with an E-scanner and a liquid cell. When inspecting dried samples, the AFM was operated in tapping mode. In this case, tapping mode silicon cantilevers TESP (Digital Instruments, Santa Barbara, CA) with nominal spring constants of 20–100 N/m and nominal resonance frequencies of 200–400 kHz were employed as described.^{33,34} When inspecting hydrated samples, the liquid cell was mounted and the microscope was operated in contact mode. Contact mode tips with a nominal spring constant of 0.06 N/m were used. The topographs were obtained at scan sizes in the range $1 \mu\text{m} \times 1 \mu\text{m}$ to $5 \mu\text{m} \times 5 \mu\text{m}$ (512×512 pixels) and flattened line by line.

2.2.5. Force spectroscopy. Force-*z*-piezo translation distance curves were obtained as described in Figure 3 using the same AFM, liquid cell and contact mode tips as for the image collection. An average adhesion force between the tip and surfaces at the various stages of the immobilisation procedure were obtained by recording force curves, including different positions on the surfaces. The surface of the sample was considered to be in contact with the tip when the output of the photodiode became a linear function of the sample displacement.³⁵

Force spectroscopy of the polysaccharide–protein interactions was carried out at room temperature unless stated otherwise. The measurements were performed in 20 mM MOPS pH 6.8, with 2 mM CaCl_2 or other divalent salts added to test divalent cations as co-factors for enzymatic activity.²² The polysaccharide-functionalised tip was brought in contact with the immobilised proteins or protein modular components by controlling the *z*-piezo movement, allowed to form substrate–active cleft interactions while remaining in contact for 100 μs , and withdrawn. In the analysis of the forced unbinding, the approach detailed by Bell³⁶ and Evans,^{6,37} which is based on Kramers' rate theory is applied. It has been shown that, under constant loading rate, the probability density $P(f)$ to observe a bond rupture of an adsorbed molecule at the force f is³⁷

$$P(f) = k^0 \exp\left(\frac{x_{\beta} f}{k_B T}\right) \exp\left[\frac{k^0 k_B T}{x_{\beta} r_f} \left(1 - \exp\left(\frac{x_{\beta} f}{k_B T}\right)\right)\right] \quad (1)$$

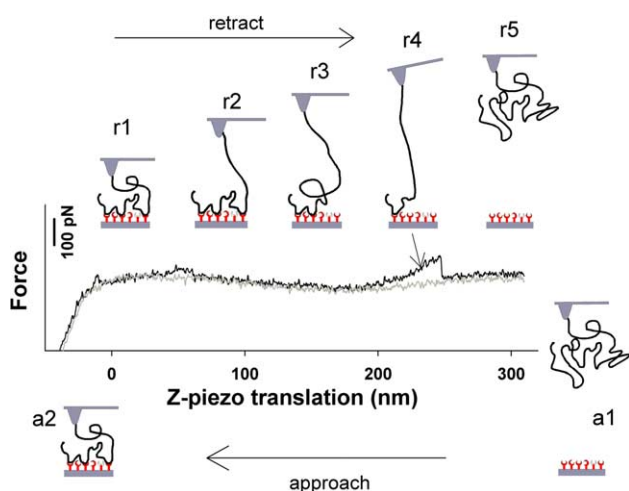


Figure 3. Schematic illustration of forced unbinding experiment on AlgE enzymes and mannuronan polysaccharides and the interpretation of characteristic features observed in the force curves. When the experiment starts, the polysaccharide-functionalised AFM tip is positioned high above the AlgE4-functionalised surface (a1). The tip is allowed to approach the surface covered with immobilised proteins by controlling the *z*-piezo movement. Continuous recording of the tip deflection gives rise to an approach curve (grey line). The surface of the sample is considered to be in contact with the tip when the output of the photodiode becomes a linear function of the sample displacement.³⁵ The polymers immobilised onto the tip are allowed to bind to active clefts on the immobilised enzymes while remaining in contact with the surface for 100 μs (a2). After this delay period, the tip is retracted from the surface (r1–r5). If a polymer–enzyme complex has formed, the polymer will, at a certain height above the surface, be pulled taut between the tip and the surface (r3–r4). This event gives rise to a deflection of the tip. The length of the polymer segment being stretched between the tip and the surface determines the position at which this happens. Upon further retraction of the tip the polymer–enzyme complex will dissociate, and the tip returns to its rest deflection (r5).

In Eq. 1, k^0 is the dissociation rate constant without an external force, x_β is the thermally averaged distance, projected along the direction of the applied force, needed to reach the transition state and $k_B T$ is the thermal energy. Recently, the parameter x_β is alternatively suggested for multiple barriers to represent the distance between the position of the lowest energy state and the rate limiting barrier at a given force-loading rate at constant force ramp.³⁸ The maximum of this distribution yields the most probable rupture force f^* . In our experiments, the tip–surface separation speed was varied between 0.1 and 5.4 $\mu\text{m/s}$. The rupture force f^* , the force-loading rate r_f and the parameter x_β were extracted from the obtained data off-line as follows.

The polymeric substrate corresponds to a flexible spacer,^{39,40} where the length of the spacer is governed by the distance between the covalent attachment to the AFM tip, and the attachment of an oligomer sequence to an enzyme. This distance can differ in each anchoring event. According to the theoretical analysis by Evans and Ritchie,³⁹ and later Monte Carlo simulations,⁴⁰ the actual force loading for each unbinding event should be taken into account. The preferred procedure for doing so involves determination of the dissociation rate and the potential width directly based on the experimental data and by using a probability density function for the rupture forces and the loading rates. The actual loading rate was determined for each force jump by use of the slope $\Delta F/\Delta t$ prior to each observed bond dissociation event. This slope was determined from a linear fit of the observed loading rate prior to the detachment event, which results in return of the cantilever to its rest position. In this way, each force jump gives rise to one observation of bond strength against loading rate, and for each tip retraction speed a certain distribution of loading rates felt by the interacting molecules are obtained. By using different tip retraction speeds, a continuously increasing distribution of loading rates is obtained. The points in the continuous distribution of loading rates were subsequently grouped into defined intervals of increasing loading rate. The mean loading rate within each sub-distribution was calculated and used as a constant when parameters x_β and k^0 were determined. Additionally, the most likely unbinding force, f^* , was obtained from this modelling. Data from hundreds of approach–retract cycles were collected, taking into account the statistical nature of a single interaction event.

3. Results and discussion

3.1. Characterisation of chemically modified coverslips

Different protocols for silanisation of surfaces have been described in the literature.^{41–44} The reaction conditions

used, that is, deposition method, duration of reaction, temperature and solvent conditions, vary considerably. The reproducibility of each step in the immobilisation procedure used in this study and the characteristics of the resulting surfaces were investigated in order to optimise the immobilisation procedure.

AFM topographs of freshly cleaved mica (Fig. 4A) indicated a mean surface roughness of 0.04 nm. Different procedures were tested in order to silanise the surface. Performing the silanisation by exposing the surface for 2 h to 10% DETA diluted in toluene heated to 120 °C, was found not to yield reproducible surface characteristics (Fig. 4B). The surface roughness varied from 0.15 to 0.37 nm. AFM topographs of the surfaces showing the highest degree of surface roughness revealed a surface morphology reminiscent of phase separation (Fig. 4B). Silanising the surface by exposing it to a solution of 1% DETA in 1 mM acetic acid for 20 min at room temperature, before rinsing in MQ-water was found to give a reproducible surface roughness (Fig. 4C, surface roughness = 0.17 nm). These experimental conditions were therefore chosen for the surface silanisation step. The silanised surfaces were exposed to a solution containing 12.5% glutaraldehyde in 0.1 M phosphate buffer, pH 6.8. Incubating the surfaces for 2 h were not sufficient in order to obtain a continuous and homogenous surface coverage (image not shown), whereas 14 h reaction time for the coupling of the glutaraldehyde yielded homogenous surfaces (Fig. 4D, surface roughness = 0.19 nm). AlgE enzymes or their modules were subsequently conjugated to the free aldehyde groups accessible on the surface. This was obtained by exposing the surface to a solution containing 50 $\mu\text{g/mL}$ AlgE enzyme-preparation in 20 mM MOPS buffer, pH 6.8 containing 2 mM CaCl_2 , incubated for 14 h at room temperature and rinsed in buffer solution. The AFM topographs obtained on these surfaces (Fig. 4E, surface roughness = 2.06 nm) or on hydrated surfaces (Fig. 4F) clearly show the presence of globular structures, previously reported to be consistent with active AlgE4.²⁸ The images of AlgE4 conjugated onto mica were compared to images of BSA conjugated onto mica using the same procedure. The mean surface roughness of the surfaces covered with immobilised BSA was 2.55 nm when imaged in liquid, and the surface had the same topology, characterised by the presence of globular structures.

The various steps of the immobilisation procedure for the functionalised mica surfaces were characterised both by adhesion properties using an uncoated Si_3N_4 AFM tip, and contact angle (Table 2). The silanisation yielded a hydrophobic surface characterised by an adhesion force of 2.4 ± 0.7 nN, and a contact angle of 52°. The surface became even more hydrophobic following the glutaraldehyde conjugation (adhesion force of 8.0 ± 1.0 nN and contact angle of 64°). The surface

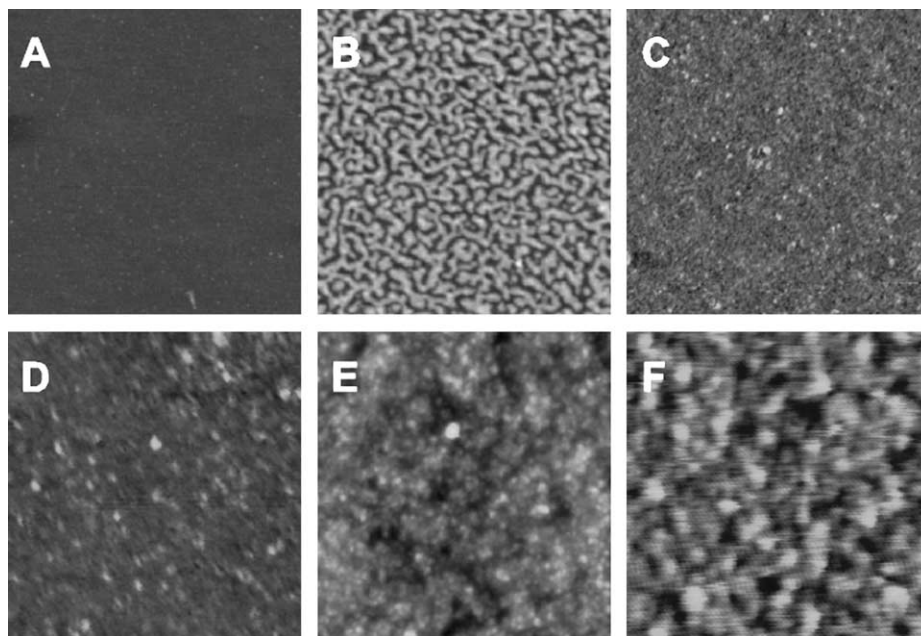


Figure 4. AFM topographs of surfaces after different surface modifications. (A) freshly cleaved mica. (B) Mica silanised by 2 h exposure to 10% DETA in toluene, heated to 120 °C. (C) Mica silanised by exposure to 1% DETA in 1 mM acetic acid for 20 min. (D) Glutaraldehyde-functionalised surface obtained by exposing the silanised surface to a solution containing 12.5% glutaraldehyde for 14 h. (E and F) Conjugation of alginate epimerase AlgE4 to functionalised mica obtained by exposing the surface to a solution containing AlgE4 for 14 h. The surface reactions giving the surfaces depicted in image C–F occurred at room temperature. Topograph A–E were obtained using tapping mode in air, topograph F was obtained using contact mode in liquid. The images correspond to a scan area of 1 µm.

Table 2. Roughness and hydrophobicity of functionalised surfaces

Surface	RMS (nm) ^a		Tip–surface adhesion ^b (nN)	Contact angle (°)
	Liquid (CM)	Air (TM)		
Cleaned mica	0.08	0.03	1.3 ± 0.8	35
Silanised mica	0.16	0.09	2.4 ± 0.7	52
Silanised mica activated with glutaraldehyde	0.74	0.13	8.0 ± 1.0	64
AlgE4 enzymes immobilised on mica	2.48	0.62	0.3 ± 0.2	95

^a The root-mean-square (RMS) surface roughness were calculated with the software provided by Digital Instruments. Frames of 750 nm scan size with number of pixels = 512 were analysed. CM and TM depict results obtained using contact mode and tapping mode, respectively.

^b The measurements were performed in aqueous 20 mM MOPS buffer solution, pH 6.8, using Si₃N₄ AFM tips.

covered with AlgE yielded 0.3 ± 0.2 nN using the untreated AFM tips, indicating a decrease in the hydrophobicity of the surface. Still, these surfaces showed an increase in the contact angle, indicating a hydrophobic surface. Partly denaturation of the enzymes, occurring in the drying step prior to the dynamic contact angle measurement can be one reason for this difference.

3.2. Observation of specific epimerase–mannuronan interactions

Figure 5A presents a gallery of force–z-piezo translation distance curves for mannuronan functionalised AFM tips interacting with immobilised AlgE6. The data reveal signatures reflecting both stretching of mannuronan and

forced unbinding between mannuronan and AlgE6 enzymes. The unbinding events occurred at tip surface separations up to about 400 nm. This distance is compatible with the chain length distribution of the mannuronan anchored to the AFM tip and that acts as a substrate for the epimerases.

The force–distance curves used in this force spectroscopy study, of which some examples are presented in Figure 5A, were obtained when using experimental conditions giving a high probability for observing single-molecular pair unbinding events.

This was achieved by adjusting the key parameters controlling the grafting density of polysaccharide on the AFM tip until a sufficiently infrequent bonding was observed. We have previously shown²⁸ that the fraction of successful anchoring events as well as the proba-

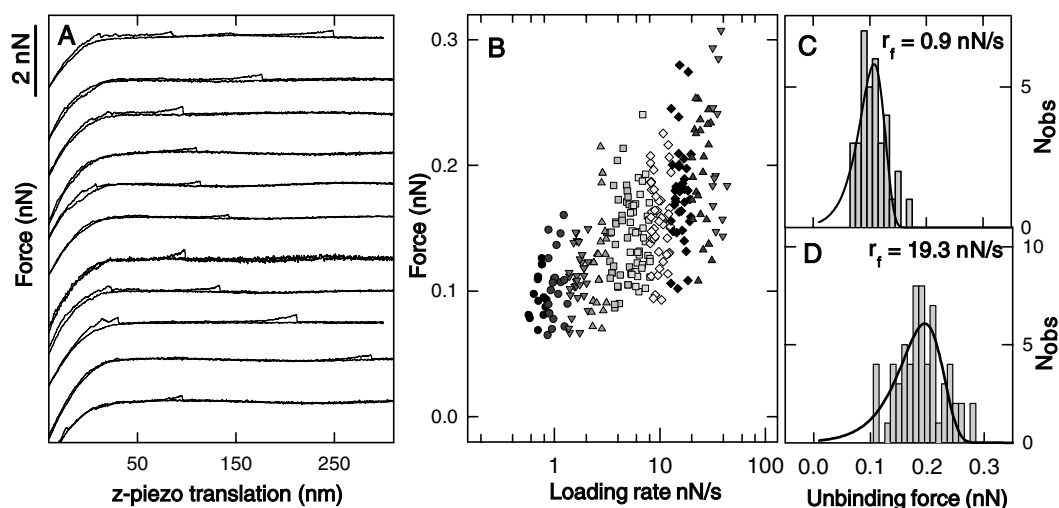


Figure 5. Steps in the analysis of the epimerase alginate substrate interaction. (A) Gallery of force–z-piezo translation distance approach and the retraction curves obtained as described in Figure 3. Most of the forced unbinding events occurred in the interval 0–300 nm, as shown in the figure, but unbinding events were observed up to 400 nm above the surface. (B) Distribution of experimentally determined mannuronan–AlgE6 unbinding forces at increasing force-loading rates. The use of different tip retraction speeds and determination of the loading rate for each force jump, as described in the text, resulted in a continuously increasing distribution of unbinding forces as a function of increasing loading rate. The data are collected from 491 force curves collected using six different tip retraction speeds. Based on the determined loading rate, the continuous distribution of observations was divided into subgroups characterised by a mean loading rate. Histograms based on the observed unbinding forces within each subgroup were generated (C and D), and x_β was determined for each subgroup. The fitted curves, from which the parameters x_β and k_0 are obtained,²⁸ are overlaid on the distributions presented in C and D. The most probable unbinding force f^* , determined from the peak in the histogram, was plotted versus increasing loading rate (Fig. 6A, D and G, large points).

bility for multiple unbinding events depended both on the concentrations of EDAC and polysaccharide used during the functionalisation procedure and the incubation time. In the present study, an EDAC concentration of 0.5 mg/mL, and a reaction time for the coupling of 2 h combined with 20 μ g/mL polysaccharide was employed in order to give a low density of polymers attached to the tip. These conditions yield anchoring in about 25% of the trials. This is somewhat in the upper range of an ideal situation, \sim 95% confidence for 1 attachment out of 10 trial touches.⁷ In view of the multiple binding sites represented by the polymer substrate for anchoring each individual chain to the enzyme, this was still considered adequate. This judgement was supported by the observed truncation of the high force tail of the distributions of unbinding forces when using this adjusted concentration of EDAC and reaction time.²⁸ The most probable unbinding forces were, therefore, determined based on distributions of unbinding forces obtained using such experimental conditions.

We have previously, by the use of various control experiments, shown that the observed interactions are specific alginate–epimerase interactions.²⁸ These control experiments included observing the absence of binding events between polyM functionalised tips and BSA on mica, or xanthan functionalised tips in combination with epimerase functionalised mica. Moreover, observations of the distance between mannuronan–AlgE4 unbinding events at various surface densities of AlgE4,

and truncation of successful anchoring events between mannuronan and AlgE4 depending on the concentration of mannuronan added as competing ligand, clearly indicated the specificity of the anchoring and associated force unbinding events. These specific interactions are further characterised by being observed at much larger separations between the AFM tip and surface, typically 100–400 nm, than the case for the adhesion mentioned above (Table 2). Signatures of adhesive interactions observed within 20 nm of the tip–substrate contact point could, therefore, be due to interactions between the surface of the tip and the functionalised mica surface, and were therefore ignored in analysis of the specific interactions.

3.3. The strength of the AlgE–mannuronan complexes

The magnitude of the external force necessary to detach AlgE enzyme–mannuronan complexes was measured at different loading rates. Based on the observations, the parameters r_f , x_β and k^0 were determined (Table 3). The observed forces are within the range determined for other lectin–carbohydrate unbinding forces. The force needed to unbind concanavalin A–oligoglucose complexes is, for example, earlier determined to be 96 ± 55 pN at a retraction rate of 0.5 μ m/s.¹¹ The difference in strength between these interactions and the strength reported for the type of covalent bonds used for the present attachments, determined to

Table 3. Estimated parameters characterising the energy-landscape of mannuronan–epimerase AlgE4, AlgE6 and their A-module

AlgE4–mannuronan				A-module–mannuronan				AlgE6–mannuronan			
$\langle r_f \rangle^a$ (nN/s)	x_β (nm)	k_0 (s ⁻¹)	f^a (pN)	$\langle r_f \rangle^a$ (nN/s)	x_β (nm)	k_0 (s ⁻¹)	f^a (pN)	$\langle r_f \rangle^a$ (nN/s)	x_β (nm)	k_0 (s ⁻¹)	f^a (pN)
0.57	0.26	0.37	73	1.1	0.07	0.46	215	0.72	0.18	0.27	108
0.86	0.20	0.67	84	1.6	0.11	0.56	249	1.0	0.20	0.26	107
1.0	0.24	0.38	86	2.4	0.13	0.54	281	1.7	0.19	0.26	121
2.4	0.31	0.25	88	3.5	0.09	0.25	299	2.7	0.14	1.12	128
4.3	0.21	0.59	98	4.9	0.09	1.1	323	6.4	0.14	1.16	151
16.3	0.18	3.1	123	6.7	0.09	1.1	344	19.3	0.11	1.80	195
24.8	0.16	3.7	141	11.8	0.06	0.7	384				
44.7	0.13	6.1	135								

The observed unbinding forces obtained at various z-piezo retraction rates were divided in intervals of force-loading rates, and the parameters for a single-barrier unbinding under constant load was obtained as described.²⁸

^a Denotes the average force-loading rate observed in the interval.

2.0 nN \pm 0.3 nN at loading rate of 10 nN/s,⁴⁵ is more than one order of magnitude.

3.3.1. AlgE4–mannuronan interactions. The most probable unbinding force, f^* , as well as the distance x_β was found to increase from 73 pN at a mean loading rate of 0.6 nN/s to 135 pN at a loading rate of 44.7 nN/s. The dynamic force spectrum (Fig. 6A) shows an increase in slope from one thermal force scale governing the strength of the interaction for loading rates up to 20 nN/s, to the next. This behaviour indicates that an outer activation barrier, located at a distance $x_\beta = 0.26$ nm from the bound complex, is suppressed at high loading rates, and that an inner barrier becomes the dominant kinetic impedance to detachment. Five different intervals of r_f , situated from 0.6 to 4.3 nN s⁻¹, located the barrier at $x_\beta = 0.24 \pm 0.04$ nm. Larger values of r_f indicated a transition into a domain determined by an inner barrier. The fits of the theoretical expression (Eq. 1) to the observed data at increasing mean unbinding force (Fig. 6B and C) was also consistent with a cascade of two energy barriers. The observed parameter values of x_β is about one third of the size of a hexopyranose residue. These are also within the range reported for other biomolecular interactions, for example, $x_\beta \approx 0.12$ nm, $x_\beta \approx 0.3$ nm and $x_\beta \approx 3$ nm for the high, intermediate and low strength regime in the case of avidin-biotin.⁷

3.3.2. AlgE6–mannuronan interactions. The strength of the AlgE6–mannuronan interaction was 108 pN at a mean loading rate of 0.72 nN/s. This increased to 195 pN at a mean loading rate of 19.3 nN/s. The strength of this complex is thus higher than that was determined for the AlgE4–mannuronan complex. The distance x_β indicated the existence of energy barriers, located at $x_\beta = 0.19$ and 0.11 nm from the bound complex. The data observed at intermediate force-loading rates may reflect a third barrier located at $x_\beta = 0.14$ nm, or alternatively a not well resolved transition from the inner to the outer barrier. The slope in the dynamic

force spectrum (Fig. 7) is consistent with the values of x_β determined for the outer and inner barrier, but does not provide additional information allowing to conclude about the intermediate region.

3.3.3. AlgE4–A-module–mannuronan interactions. The unbinding force was for this complex larger than that for the AlgE4– and AlgE6–mannuronan complexes, and increased from 215 pN at a mean loading rate of 1.1 nN/s (Fig. 6H) to 385 pN at $r_f = 11.8$ nN/s (Fig. 6I). The strength of this complex was also more dependent on the loading rate than the AlgE–mannuronan complexes. The data in the dynamic force spectrum (Fig. 6G) were consistent with a single energy barrier located at $x_\beta = 0.10$ nm. The distance x_β indicated an average distance x_β equal to 0.1 ± 0.02 nm over the whole interval of loading rates.

3.3.4. R-module–mannuronan interactions. Force curves obtained when mannuronan-labelled tips were retracted from a layer of R-modules immobilised on mica did not contain signatures reflecting polymer anchoring. This finding is consistent with the hypothesis that the A-module contains the alginate binding site.²² The reduced binding strength of the AlgE4–mannuronan interaction compared to the A-module–mannuronan interaction suggests a function of the R-module related to regulation of the enzyme–substrate binding strength.

The data indicate that when no strong forces are acting on the enzyme–substrate complex, corresponding to the situation when the molecules are interacting in solution, the dominant kinetic impedance to detachment is located at $x_\beta = 0.09$ nm for the A-module, increasing to $x_\beta = 0.19$ nm for AlgE6 and 0.26 nm for AlgE4. Different hypothesis exists regarding the function of the R-module. It has been proposed to be a source of Ca²⁺ for the catalytic part (the A-module), or to stimulate binding of the epimerase to the substrate.¹⁹ The present data suggest that the distance separating the active site-substrate from the activation barrier to be crossed, as well as the strength of the bond keeping the enzyme-sub-

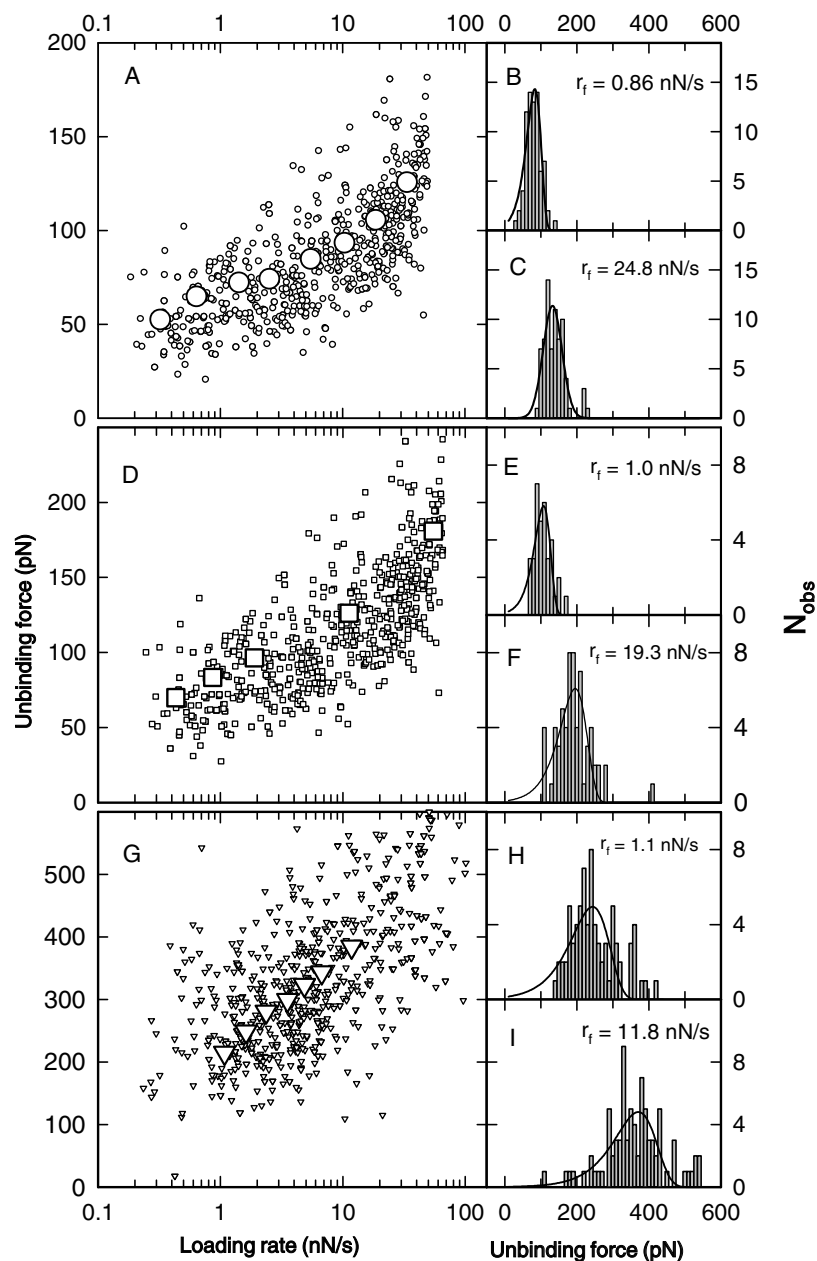


Figure 6. Distribution of experimentally determined mannuronan-epimerase AlgE4 (A–C), mannuronan-epimerase AlgE6 (D–F), and mannuronan-epimerase AlgE4 *A*-module (G–I) unbinding forces at increasing force-loading rates and most probable unbinding force versus load with increasing loading rate. The data are collected from 2640 force curves obtained using five different tip retraction speeds in the interval 0.2–4 $\mu\text{m/s}$ (A, D and G, small points). Histograms based on the observed unbinding forces within each subgroup of unbinding events were generated (AlgE4: B,C; AlgE6: E,F; *A*-module: H,I), and parameter x_β determined. Dynamic force spectra were obtained by plotting the most probable unbinding force f^* , determined from the peak in the histogram, versus \log_e (loading rate) (A, D and G, large points).

strate complex together, are modulated by the presence of the R-module.

3.4. The life-time of the AlgE-mannuronan interactions

The value of k^0 obtained when extrapolating the most probable unbinding force to zero force, $f^* = 0$, giving $k^0 = r_f x_\beta / k_B T$,⁴⁶ (Fig. 7) reflect the off-rate of the proteins at zero force-loading rate. This value is equal to

the thermal off-rate in solution,⁴⁶ referred to as k_{off} . Applying this procedure, we determined the value of k_{off} to be 0.37 s^{-1} for AlgE4, 0.23 s^{-1} for AlgE6 and 0.85 s^{-1} for the *A*-module. The values of k^0 were obtained as previously described,²⁸ 0.37 s^{-1} , 0.27 s^{-1} and 0.56 s^{-1} for the AlgE4, AlgE6 and *A*-module-mannuronan interactions, respectively, are in the same range as the values obtained for k_{off} (Table 2). An estimate for the catalytic constant, k_{cat} , the maximum number of substrate

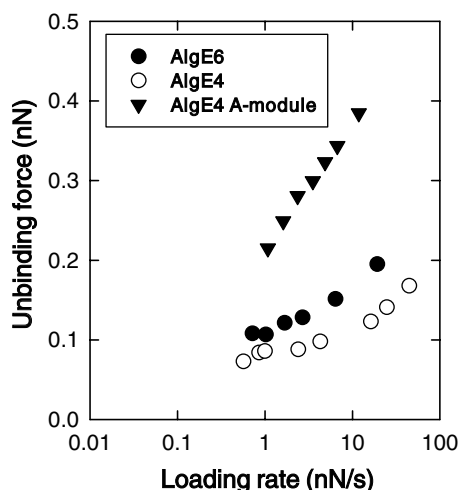


Figure 7. Dynamic strength spectra for AlgE4-mannuronan (open circles), AlgE6-mannuronan (closed circles) and A-module-mannuronan interactions (closed triangles). Defined as thermal energy $k_B T$ /distance x_β , the slope of the linear regimes seen in the dynamic spectra (discontinuous lines) map activation barriers at positions along the direction of force.

molecules converted to product per active site per unit time, has been reported for AlgE4, and the value reported or 14 s^{-1} in aqueous solution at 37°C .²² Such information about k_{cat} is not yet available for AlgE6 or the A-module. For AlgE4 this yields a mean enzyme-mannuronan residence time of about 0.07 s per epimerised uronide. Comparison of k_{cat} with k^0 and k_{off} suggest that the average duration of the polymer-enzyme interaction is much in excess of the average duration of single epimerisation. The latter is calculated to 0.2 s for AlgE4-mannuronan, as estimated from the experimental value $k_{\text{cat}} = 14 \text{ s}^{-1}$ and corrected for the difference in temperature. This supports several single ManpA epimerisations per unbinding event indicative of a processive mode of action of AlgE4 acting on mannuronan. An additional indication for a processive mode of action of AlgE4 is implicit in the observation of unbinding events between mannuronan and AlgE4, AlgE6 or their A-module occurring up to a polymer segment length of about 400 nm at the slowest retraction rate. These unbinding events point towards a polymer-enzyme residence time two orders of magnitude longer than the time needed for AlgE4 to epimerise a single residue.

Similar force-unbinding studies were carried out using the hybrid epimerase PKA1 composed of subunits from AlgE4 and AlgE2.²⁷ This enzyme yields a random sequence in the product most likely due to a random attack mechanism and dissociation between the chain and PKA1 following each epimerisation. The finding that the PKA1-mannuronan unbinding events only occurred up to a substrate-mannuronan tip separation less than 50 nm (retraction speed $v_{\text{ret}} \leq 0.4 \mu\text{m/s}$) suggests a much higher dissociation rate of mannuronan-PKA1 complexes compared to mannuronan-AlgE

complexes. The data from the AFM experiments show a clear distinction between the two enzymes, AlgE4 and PKA1, most probably arising from their different mode of action.

3.5. Observations of AlgE4-polyMG alginate interactions

Force-z-piezo translation distance curves collected for polyalternating (polyMG) alginate functionalised AFM tips interacting with AlgE4 immobilised on mica showed signatures indicating multiple unbinding events and unbinding forces in the range 0.1–3 nN (Fig. 8A, upper curves). Reduction of the tip graft density of polyMG alginate by reducing the incubation time from 2 h to 30 min for the coupling reaction resulted in a decreased probability for anchoring events, but did not increase the probability for single unbinding events significantly. The use of mica surfaces incubated in a mixture of BSA and AlgE4 resulted in a greatly increased probability of single unbinding events (Fig. 8A, lower curves) compared to that was observed when using surfaces coated with AlgE4. The strength of the AlgE4-polyalternating alginate interactions was in the same range as observed for the AlgE4-mannuronan interaction (Fig. 8B). The polymer chain stiffness of alginate blocks increases in the order $\text{MG} < \text{MM} < \text{GG}$.⁴⁷ The larger chain flexibility of polyMG alginate compared to mannuronan may thus explain the observed differences in behaviour between the two polymers in this interaction study. The higher flexibility of polyMG alginate might give rise to an increased ability, compared to mannuronan, to bind to several immobilised enzymes. Thus, it is necessary to increase the distance between the active enzymes when using a polyMG alginate labelled AFM-tip in order to observe single unbinding events.

Polyalternating alginate is the end product when AlgE4 is working on mannuronan. The observed long stability of the AlgE4 polyalternating alginate complex, indicates that the enzyme can bind polyalternating alginate. In a previous study of time progress curves for AlgE4 working on mannuronan, a scenario where the product (polyalternating alginate) functions as a competitive inhibitor, was proposed as a mechanism that could explain the observations.⁴⁸ Interestingly, such an ability of the enzyme to bind polyalternating alginate is a necessary prerequisite for processivity.

3.6. The lifetime of the interaction between AlgE4 and naturally occurring alginate

Figure 8C presents some characteristic force z-piezo translation distance curves obtained when AFM tips labelled with alginate extracted from an algae (incubation time: 2 h) were retracted from mica covered with AlgE4. A high number of unbinding events were observed with-

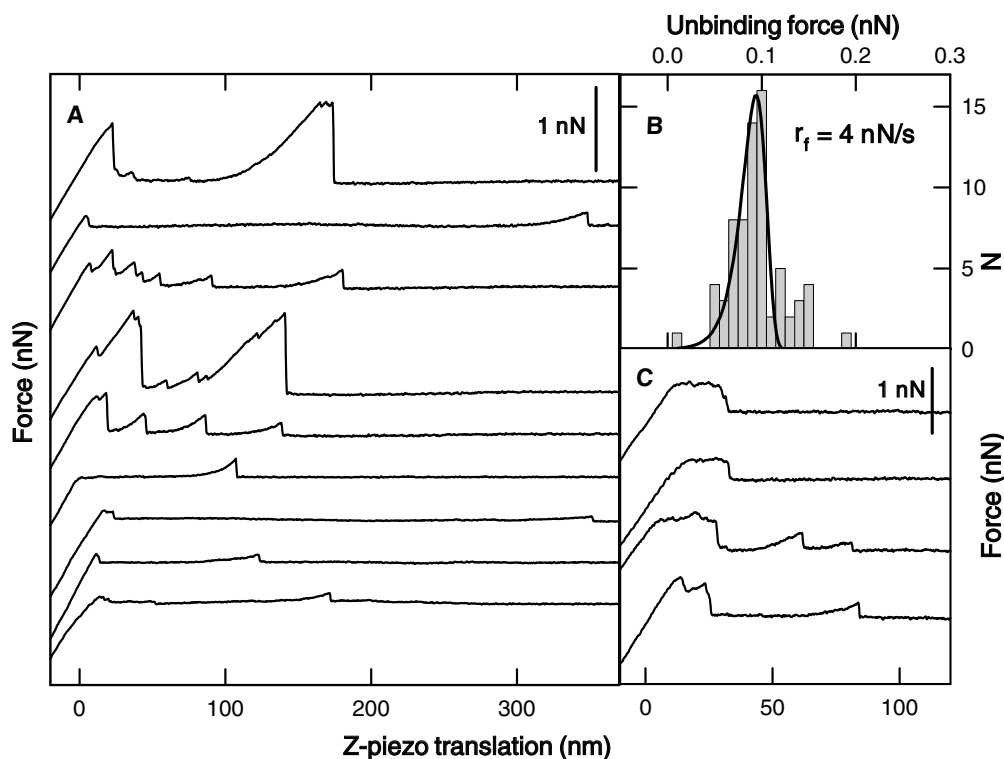


Figure 8. (A) Gallery of force–z-piezo translation distance curves obtained for polyMG alginate functionalised AFM tips (incubation time: 2 h) interacting with AlgE4 immobilised on a solid support. Nearly all trials resulted in multiple unbinding events and unbinding forces in the range 0.1–3.0 nN (five upper curves). Diluting the AlgE4 preparation with BSA (1:9) prior to the conjugation step resulted in a greatly increased probability of single unbinding events and disappearance of forces above 1 nN (four lower curves). (B) Distribution of polyMG–AlgE4 unbinding forces using the experimental conditions explained for the four lower curves and a loading rate equal to 4 nN/s. (C) Gallery of force–z-piezo translation distance curves obtained when retracting tips labelled with commercial alginate (incubation time: 2 h) from mica covered with AlgE4. A high number of unbinding events were observed to occur 0–30 nm above the mica surface, whereas no unbinding events were observed in a distance above the surface greater than 80 nm (lower curve).

in the interval 0–30 nm above the mica surface. In this region of the curve signatures reflecting hydrophobic or other non-specific interactions between the tip and the surface will appear, if present. This makes it difficult to distinguish between unbinding events and unspecific interactions. Such hydrophobic interactions were weak if present at all in curves obtained when using mannuronan- or polyMG alginate labelled AFM-tips. This fact, together with the saw-tooth like shape of the retraction curve, points towards the interpretation that the observed interactions reflect forced unbinding of AlgE4–alginate complexes rather than unspecific hydrophobic interactions. The increased probability for the unbinding events to occur close to the mica surface indicates a higher probability for short-lived interactions, dissociating within the time interval needed to rise the tip high above the surface. No unbinding events were observed in a distance above the surface greater than 80 nm. With the tip retraction speed used, this distance corresponds to an AlgE4–alginate complex lifetime of 0.2 s. The short lifetime of this interaction compared to the lifetime observed for AlgE4–mannuronan or AlgE4–polyalternating alginate interactions can be due to the chemical composition of the alginate used. A processive nature

of AlgE4 combined with an inability or decreased ability of this one to bind G-blocks might result in dissociation of the enzyme–substrate complex upon entrance of a G block into the enzyme active site.

3.7. Cation dependence of epimerase–alginate interactions

All the AlgE epimerases are dependent on Ca^{2+} for activity, but earlier studies have shown that Sr^{2+} is able to substitute for Ca^{2+} although the efficiency of the enzyme is decreased to about 30%.²² In the same study, it was concluded that Mg^{2+} , Mn^{2+} , Ba^{2+} and Zn^{2+} did not have any stimulatory effect on the epimerisation reaction in the absence of Ca^{2+} . At optimal Ca^{2+} concentration, all ions tested (except Mg^{2+}) were inhibitory. In an attempt to study this further, the complex formation between AlgE4 and mannuronan was studied in the presence of the divalent cations Ca^{2+} , Sr^{2+} , Mg^{2+} , Ba^{2+} and Zn^{2+} . All the ions were added to a concentration equal to 1.5 mM, using chloride as anion. From the force curves, it could be concluded that binding occurred in all cases and no apparent difference in binding frequency was observed among the different ions. The interaction was also determined in absence of ions

(MOPS pH 6.8). In this case the force curves did not contain any signatures reflecting unbinding events, indicating that the probability of forming mannuronan–AlgE4 complexes is greatly reduced in ion-free buffer solution. When reintroducing monovalent cations (Na^+ , 1.5 mM), force jumps were immediately observed. Based on these observations we conclude that complex formation between mannuronan and AlgE4 is dependent on cations, but both monovalent and divalent ions make complex formation possible. The first step in the proposed mechanism for alginate epimerases is neutralisation of the negatively charged mannuronic acid residue.⁴⁹ The observations indicate that any cation among the ones studied make this binding step possible. This is in contrast to the second step in the proposed mechanism, that is, the epimerisation reaction. In earlier studies on the activity of AlgE4 in the presence of different cations, it was concluded that the epimerisation process necessitates the presence of either Ca^{2+} or Sr^{2+} .²²

4. Conclusions

Dynamic force spectroscopy was used to measure the unbinding forces between a polysaccharide and a non-degrading enzyme. The experimental procedure used involves immobilisation of the interacting molecules. AFM imaging and force curves, as well as dynamic contact angle measurements proved to be useful tools, revealing the effect and reproducibility of different surface treatment procedures. Analysis of the force profiles gave insight into the process of enzyme binding and unbinding, as well as the mode of action of the enzyme. The results show that for AlgE4 and AlgE6, the position of the activation barrier and the strength of the epimerase–substrate interaction at low detachment force are influenced by the presence of the R-module component. This indicates a possible function of the R-module related to regulation of the interaction strength. The observed ability of AlgE4 to bind polyMG alginate is consistent with a mechanism of product inhibition. In addition, the observed cation dependence of the enzyme–substrate binding process illustrates a potential of AFM force spectroscopy to offer new insight into biochemical processes. The evidence of a processive mode of action of AlgE4, based on the ratio between off-rates at zero force and rate for epimerisation of β -D-ManpA residues, indicates that enzymes with a processive mode of action also exist for non-degrading polysaccharide modifying enzymes.

Acknowledgements

We thank Svein Valla for helpful discussions concerning the AlgE-epimerases, Tonje Bjerkan and Finn Aach-

mann for providing the A- and R-modules as well as the PKA1 enzyme, and Gisle Øye for assistance with the dynamic contact angle measurements. This work was supported by the Norwegian Research Council Grant No. 145523/432 and by the European Commission Grant No. QLK 3-CT 1999 00034.

References

- Gélinas, S.; Finch, J. A.; Vreugdenhil, A. J. *Colloid Surf. A* **2000**, *164*, 257–266.
- Tiner, W. J.; Potaman, V. N.; Sinden, R. R.; Lyubchenko, Y. L. *J. Mol. Biol.* **2001**, *314*, 353–357.
- Butt, H. J.; Wolff, E. K.; Gould, S. A. C.; Northern, B. D.; Peterson, C. M.; Hansma, P. K. *J. Struct. Biol.* **1990**, *105*, 54–61.
- Smith, D. A.; Connell, S. D.; Robinson, C.; Kirkham, J. *Anal. Chim. Acta* **2003**, *479*, 39–57.
- Gad, M.; Itoh, A.; Ikai, A. *Cell Biol. Int.* **1997**, *21*, 697–706.
- Evans, E. *Annu. Rev. Biophys. Biomol. Struct.* **2001**, *30*, 105–128.
- Evans, E. *Faraday Discuss.* **1998**, *111*, 1–16.
- Rief, M.; Clausen-Schumann, H.; Gaub, H. E. *Nat. Struct. Biol.* **1999**, *6*, 346–349.
- Florin, E.-L.; Moy, V. T.; Gaub, H. E. *Science* **1994**, *264*, 415–417.
- Hinterdorfer, P.; Baumgartner, W.; Gruber, H. J.; Schilcher, K.; Schindler, H. *Proc. Natl. Acad. Sci. U.S.A.* **1996**, *93*, 3477–3481.
- Touhami, A.; Hoffmann, B.; Vasella, A.; Denis, F. A.; Dufrene, Y. F. *Langmuir* **2003**, *19*, 1745–1751.
- Bucior, I.; Scheuring, S.; Engel, A.; Burger, M. *J. Cell Biol.* **2004**, *165*, 529–537.
- Hertadi, R.; Gruswitz, F.; Silver, L.; Koide, A.; Koide, S.; Arakawa, H.; Ikai, A. *J. Mol. Biol.* **2003**, *333*, 993–1002.
- Persike, N.; Pfeiffer, M.; Guckenberger, R.; Radmacher, M.; Fritz, M. *J. Mol. Biol.* **2001**, *310*, 773–780.
- Moe, S. T.; Draget, K. I.; Skjåk-Bræk, G.; Smidsrød, O. Alginate. In *Food Polysaccharides and their Applications*; Stephen, A., Ed.; Marcel Dekker: NY, 1995; pp 245–286.
- Ertesvåg, H.; Høidal, H. K.; Schjerven, H.; Glærum Svanem, B. I.; Valla, S. *Metab. Eng.* **1999**, *1*, 262–269.
- Svanem, B. I. G.; Skjåk-Bræk, G.; Ertesvåg, H.; Valla, S. *J. Bacteriol.* **1999**, *181*, 68–77.
- Ertesvåg, H.; Skjåk-Bræk, G. Modification of alginate using mannuronan C-5-epimerases. In *Methods in Biotechnology*, Bucke, C., Ed.; Humana Press, Totowa NJ, 1999; pp 71–78.
- Ertesvåg, H.; Valla, S. *J. Bacteriol.* **1999**, *181*, 3033–3038.
- Ertesvåg, H.; Høidal, H. K.; Hals, I. K.; Rian, A.; Doseth, B.; Valla, S. *Mol. Microbiol.* **1995**, *16*, 719–731.
- Salmivirta, M.; Lidholt, K.; Lindahl, U. *FASEB J.* **1996**, *10*, 1270–1279.
- Høidal, H. K.; Ertesvåg, H.; Skjåk-Bræk, G.; Stokke, B. T.; Valla, S. *J. Biol. Chem.* **1999**, *274*, 12316–12322.
- Campa, C.; Holtan, S.; Nilsen, N.; Bjerkan, T. M.; Stokke, B. T.; Skjåk-Bræk, G. *Biochem. J.* **2004**, *381*, 155–164.
- Christensen, B. E.; Ulset, A.-S.; Beer, M. U.; Knuckles, B. E.; Williams, D. L.; Fishman, M. L.; Chau, H. K.; Wood, P. J. *Carbohydr. Polym.* **2001**, *45*, 11–21.

25. Fredheim, G. E.; Braaten, S. M.; Christensen, B. E. *J. Chromatogr. A* **2002**, *942*, 191–199.
26. Oberhauser, A. F.; Badilla-Fernandez, C.; Carrion-Vazquez, M.; Fernandez, J. M. *J. Mol. Biol.* **2002**, *319*, 433–447.
27. Bjerkan, T. M.; Lillehov, B. L.; Strand, W. I.; Skjåk-Bræk, G.; Valla, S.; Ertesvåg, H. *Biochem. J.* **2004**, *381*, 813–821.
28. Sletmoen, M.; Skjåk-Bræk, G.; Stokke, B. T. *Biomacromolecules* **2004**, *5*, 1288–1295.
29. Ludwig, M.; Dettmann, W.; Gaub, H. E. *Biophys. J.* **1997**, *72*, 445–448.
30. Wang, H.; Bash, R.; Yodh, J. G.; Hager, G. L.; Lohr, D.; Lindsay, S. M. *Biophys. J.* **2002**, *83*, 3619–3625.
31. Yang, B.; Yang, B. L.; Goetinck, P. F. *Anal. Biochem.* **1995**, *228*, 299–306.
32. Florin, E.-L.; Rief, M.; Lehmann, H.; Ludwig, M.; Dornmair, C.; Moy, V. T.; Gaub, H. E. *Biosens. Bioelectron.* **1995**, *10*, 895–901.
33. Stokke, B. T.; Falch, B. H.; Dentini, M. *Biopolymers* **2001**, *58*, 535–547.
34. Maurstad, G.; Danielsen, S.; Stokke, B. T. *J. Phys. Chem. B* **2003**, *107*, 8172–8180.
35. Ducker, W. A.; Senden, T. J.; Pashley, R. M. *Langmuir* **1992**, *8*, 1831–1836.
36. Bell, G. I. *Science* **1978**, *200*, 618–627.
37. Evans, E.; Ritchie, K. *Biophys. J.* **1997**, *72*, 1541–1555.
38. Derenyi, I.; Bartolo, D.; Ajdari, A. *Biophys. J.* **2004**, *86*, 1263–1269.
39. Evans, E.; Ritchie, K. *Biophys. J.* **1999**, *76*, 2439–2447.
40. Friedsam, C.; Wehle, A. K.; Kühner, F.; Gaub, H. E. *J. Phys.: Condens. Matter* **2003**, *15*, S1709–S1723.
41. Bae, A.-H.; Lee, S.-W.; Ikeda, M.; Sano, M.; Shinkai, S.; Sakurai, K. *Carbohydr. Res.* **2004**, *339*, 251–258.
42. Elender, G.; Kühner, M.; Sackmann, E. *Biosens. Bioelectron.* **1996**, *11*, 565–577.
43. Vinckier, A.; Heyvaert, I.; D’Hoore, A.; McKittrick, T.; Van Haesendonck, C.; Engelborghs, Y.; Hellemans, L. *Ultramicroscopy* **1995**, *57*, 337–343.
44. Lambert, A. G.; Neivandt, D. J.; McAloney, R. A.; Davies, P. B. *Langmuir* **2000**, *16*, 8377–8382.
45. Grandbois, M.; Beyer, M.; Rief, M.; Clausen-Schaumann, H.; Gaub, H. E. *Science* **1999**, *283*, 1727–1730.
46. Schwesinger, F.; Ros, R.; Strunz, T.; Anselmetti, D.; Güntherodt, H.-J.; Honegger, A.; Jermutus, L.; Tiefenauer, L.; Plückthun, A. *Proc. Natl. Acad. Sci. U.S.A.* **2000**, *97*, 9972–9977.
47. Smidsrød, O.; Glover, R. M.; Whittington, S. G. *Carbohydr. Res.* **1973**, *27*, 107–118.
48. Hartmann, M.; Holm, O. B.; Johansen, G. A. B.; Skjåk-Bræk, G.; Stokke, B. T. *Biopolymers* **2002**, *63*, 77–88.
49. Gacesa, P. *FEBS Lett.* **1987**, *212*, 199–202.